Received October 2, 2019, accepted October 29, 2019, date of publication November 11, 2019, date of current version November 27, 2019.

*Digital Object Identifier 10.1109/ACCESS.2019.2952999*

# Fiber-Optic Auditory Nerve of Ground in the Suburb: For Traffic Flow Monitoring

**SHENG LIANG[1], XIAOTING ZHAO[1], RUIJUN LIU[2], XIAODONG ZHANG[3], LIANG WANG[3], XINGHUA ZHANG[1], YISHENG LV[4], AND FANCHAO MENG[1]**

[1]Key Laboratory of Education Ministry on Luminescence and Optical Information Technology, National Physical Experiment Teaching Demonstration Center, Department of Physics, School of Science, Beijing Jiaotong University, Beijing 100044, China
[2]School of Computer and Information Engineering, Beijing Technology and Business University, Beijing 100048, China
[3]Beijing Municipal Institute of City Planning and Design (BICP), Beijing 100045, China
[4]State Key Laboratory for Management and Control of Complex Systems, Institute of Automation, Chinese Academy of Sciences, Beijing 100190, China

Corresponding authors: Ruijun Liu (liuruijun@btbu.edu.cn) and Xiaodong Zhang (zhangxd@bgy.cn)

This work was supported in part by the Beijing Natural Science Foundation under Grant 4192047, in part by the Fundamental Research Funds for the Central Universities under Grant 2018JBM070, and in part by the National Natural Science Foundation of China under Grant 61675019.

**ABSTRACT** We propose a novel fiber-optic auditory nerve of ground (FANG) in the suburb based on the fiber-optic distributed vibration sensor (DVS). The feasibility and effectiveness of the principle prototype FANG for traffic flow monitoring are proved and investigated by the field experiment. One of the 31.8 km-long redundant optical fiber of the buried optical-fiber cable for data transmission is utilized as the sensing fiber. Then, the phase-sensitive optical time-domain reflectometer ($\varphi$-OTDR) based DVS is realized and regarded as the FANG. The vibration events at 9 observation points with different ground conditions along the sensing fiber are detected by a threshold algorithm during 6.5 hours from 8:00 am. Then, the vibration events are analyzed in combination with the ground conditions to recognize the machine working in the factory, rammer working and the vehicles passed through near different areas and roads. The traffic flow is estimated by the vibration-counting with a counting error that is believed to be in an acceptable range. The distribution and the fluctuation trends of the estimated traffic flow are useful and enlightening for the traffic monitoring and pre-warning of special events, such as an accident. The accuracy can be improved by artificial intelligence methods in the future. It seems that our proposed FANG can be a potential and effective tool for the internet of things, smart ground and smart traffic in the suburb where the video and other information collection methods are not available.

**INDEX TERMS** Fiber-optic distributed vibration sensor (DVS), fiber-optic nerve of ground, $\varphi$-OTDR, smart ground, Internet of Things (IoT), smart traffic, traffic flow.

## I. INTRODUCTION

Nowadays, the smart applications, such as smart city, smart traffic, smart ground and smart grid, have attracted a tremendous amount of interests [1]–[7]. They are all fundamentally supported by the internet of things (IoT) to connect everything by the sensing techniques [1]–[7].

The smart traffic is one of the fastest-growing fields of the smart applications. The monitoring [8]–[18], forecasting [19]–[29], and management [30]–[32] of the traffic flow have been investigated by different methods for the smart traffic, as shown in Table 1.

The associate editor coordinating the review of this manuscript and approving it for publication was Huimin Lu.

It is necessary to achieve the sensing before the connection to realize the IoT. Therefore, the monitoring of traffic flow is the premise of effectuating smart traffic.

A great deal of sensing and detecting methods, including 5G cellular network and RFID [8], fixed and UAV loaded videos [9], [10], internet data such as social media texts [11], magnetic sensor for measurement of earth's magnetic field changes [12] and the collection of toll ticket data [13], have been proposed to detect and estimate the traffic flow. Then, different algorithms and data-analysis methods can be utilized to estimate [14]–[18], forecast [19]–[29] and measure [30]–[32] the traffic flow, which is all based on the monitoring of traffic flow by the sensing and data acquisition.

**TABLE 1.** Some current works on smart traffic.

| Ref. | Work | Method |
|---|---|---|
| [8] | monitoring of traffic flow | 5G cellular network and RFID |
| [9] | monitoring of traffic flow | edge-computing video analytics |
| [10] | monitoring of traffic flow | UAV video |
| [11] | monitoring of traffic flow | social media texts |
| [12] | monitoring of traffic flow | sensing of earth's magnetic field changes |
| [13] | monitoring of traffic flow | collection of toll ticket data |
| [14] | monitoring of traffic flow | vehicle tracking algorithm |
| [15] | monitoring of traffic flow | data plane using P4 |
| [16] | monitoring of traffic flow | accident recognition via 3D CNNs |
| [17] | monitoring of traffic flow | adapted $K$-nearest neighbors |
| [18] | monitoring of traffic flow | empirical observations and formulations |
| [19] | prediction of traffic flow | improved wavelet neural network |
| [20] | prediction of traffic flow | fitting data to optimize prediction model |
| [21] | prediction of traffic flow | exponential smoothing and learning machine |
| [22] | prediction of traffic flow | adaptive multi-Kernel SVM |
| [23] | prediction of traffic flow | generative adversarial framework |
| [24] | prediction of traffic flow | HTM and LSTM |
| [25] | prediction of traffic flow | machine learning |
| [26] | prediction of traffic flow | neural networks |
| [27] | prediction of traffic flow | hybrid dual Kalman filtering model |
| [28] | prediction of traffic flow | long short-term memory with attention mechanism |
| [29] | prediction of traffic flow | layerwise structure and Markov transition matrix |
| [30] | management of traffic flow | video and image processing based IoT |
| [31] | management of traffic flow | RFID |
| [32] | management of traffic flow | deep learning |
| This work | monitoring of traffic flow | fiber-optic auditory nerve of ground (FANG) |

However, without video monitoring, other information collections are also difficult for the smart applications in the suburbs far away from the city.

It is the fiber-optic distributed sensor that brings the opportunity to solve this problem. In the suburbs, there may be long optical fiber cables buried underground for the optical telecom network or along with the oil and gas pipelines for data transmission. In fact, the optical fiber is not only a transmission medium for communication but also a material that can be used as a sensor as well.

The installed telecom optical fiber has been employed in the giant fiber-optic gyroscopes for the angular velocity measurement with the ultra-high sensitivity [33], [34]. The optical fiber of the metropolitan optical networks can also be utilized for the fiber Bragg grating (FBG) as the sensing element to realize the three-axes accelerometer measurement, water-level, rainfall and traffic-monitoring of the smart city [35]. However, this work, which is high-cost and difficult for the areas in the suburb, requires the interventional refitting of the existing fibers to connect the FBG sensing elements.

The telecom optical fiber can also be used as the sensing fiber of the fiber-optic distributed vibration sensor (DVS), which can detect and locate the vibration along the long sensing fiber. DVS has been utilized for the applications, including intruder detection, pipelines monitoring, earthquake detection, railway and health monitoring of civil structure [36]–[57]. The phase-sensitive optical time-domain reflectometer ($\varphi$-OTDR) has been proved to be an efficient way of DVS for smart applications because of the simple installation with only one optical fiber, fast response and high sensitivity [36]–[57].

The installed telecom optical fibers based DVS have been proposed for the earthquake observations [58] and the traffic monitoring, including the vehicle speed, density, and road conditions estimation [59]. The work reported in [59] is an enlightening investigation on the DVS for applications to the smart city with the help of the artificial intelligence (AI). However, this work provides the traffic flow and the average speed of a few selected positions with the high SNR (signal-to-noise ratio) owing to the relatively ideal cable position and ground condition. The results are calibrated with the video analytics by AI, which is not feasible in suburbs.

DVS can be considered as the auditory nerve of the ground to "hear" the vibration events. In this paper, we use the fiber-optic cables based DVS to realize that geoauditory nerve can "hear the vibration" on the ground in the suburbs, where the visual nerve (video) is not available.

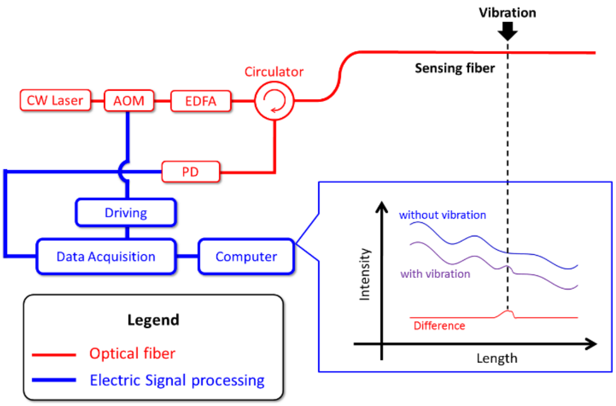


**FIGURE 1.** The schematic diagram of $\varphi$-OTDR based fiber-optic DVS.

## II. DVS BASED FANG

The experiment setup of our proposed FANG by the $\varphi$-OTDR based fiber-optic DVS is shown in Fig. 1. A highly coherent continuous laser with the narrow linewidth of $\sim$10 kHz is employed to enhance the coherent effects of the Rayleigh back-scattered light rather than to avoid them in a conventional OTDR. The continuous light with wavelength of 1550.5 nm generated from the laser is modulated by an acousto-optic modulator (AOM) into the pulsed light with a pulse width of WP $\approx$ 500 ns. Then, the light pulse is amplified by an erbium-doped fiber amplifier (EDFA) and launched into the single-mode sensing fiber through a circulator. Then, the Rayleigh back-scattered light is detected by a photodetector (PD) and converted into the digital signal by the analog-digital converter in the data acquisition. Finally, the digital signal is collected into the computer.

When there is a vibration event around the sensing fiber, the dynamic strain induced by vibration changes the refractive index and the fiber length at the effecting position. Therefore, there will be a phase difference between the Rayleigh back-scattered light, and the light intensity traces will fluctuate at the corresponding position due to the interference. Then, the vibration can be detected and located by the trace-to-trace intensity demodulation.

The vibration position can be obtained by the time when the pulse arrives back at the PD. The time delay corresponding to the peak point of the intensity difference curve has a following relationship with distance $L$ of the sensing fiber, which can be expressed as:

$$\tau = 2nL/c \tag{1}$$

where $n$ refers to the effective refractive index of the fundamental mode in optical fiber, and $c$ refers to the light speed in vacuum. The spatial resolution $\Delta z$ of $\varphi$-OTDR depends on the width of the input pulse $W_P$, which can be shown as:

$$\Delta z = cW\mathrm{p}/2n \tag{2}$$

In our experiment, the spatial resolution is $\Delta z \approx 50$ m corresponding to $W_P \approx 500$ ns.

Therefore, the sensing fiber can be divided into several effective sensing zones with the length of $\Delta z$. For a vibration event, at the position of fiber length $L$, the position can be obtained in the $N^{\text{th}}$ zone:

$$N = [L/\Delta z] + 1 \tag{3}$$

The symbol $[\sim]$ refers to the operation of rounding toward zero.

In order to achieve the judgment of vibration events and remove the influences of the noises, the threshold of the determination for vibration event can be obtained by several different signal processing and AI methods. When the difference of back-scattered light intensity exceeds the threshold, the vibration can be determined and the position can be obtained by calculating the number of sensing zone by (3).

## III. TRAFFIC FLOW MONITORING BY FANG

The FANG by $\varphi$-OTDR based DVS is implemented by only one of the redundant fibers in the existing optical fiber cable for data transmission with the length of 31.8 km. The cable is buried at depth of 0.8~1.5 m. The map for the field test of FANG based on the existing optical fiber cable is shown in Fig. 2.

We chose 9 positions in different sensing zones along the sensing fiber, as illustrated in Fig. 2. These chosen positions are at the both ends of the sensing fiber, because it is available to observe the ground conditions without the help of videos.

The fluctuation of back-scattered light intensity is detected and the difference is obtained by a one second trace-to-trace recording. The differences at different positions ($D_i$) are normalized by the maximal value of the differences ($D_{max}$) of all positions along the entire sensing fiber.

$$D_{Ni} = D_i/D_{max} \tag{4}$$

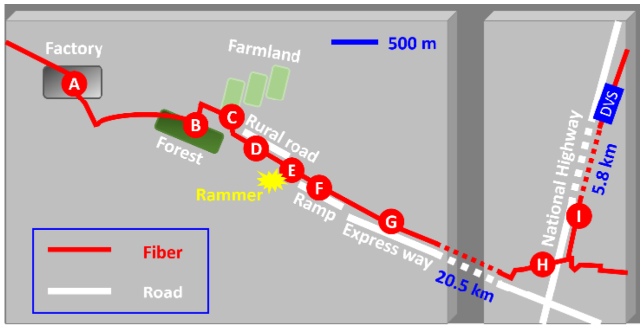


**FIGURE 2.** The map for field test of FANG formed on the basis of 31.8 km-long existing optical fiber cable.

**TABLE 2.** Ground conditions of some chosen positions.

| Ground Conditions | Position | Fiber length (km) |
|---|---|---|
| passing through a factory | A | 31.10 |
| passing through a forest | B | 29.95 |
| near a farmland | C | 29.45 |
| near a rural road | D | 29.05 |
| near a working rammer | E | 28.60 |
| near a ramp | F | 28.20 |
| along an express way | G | 27.40 |
| passing through a national highway | H | 6.50 |
| along a national highway | I | 5.85 |

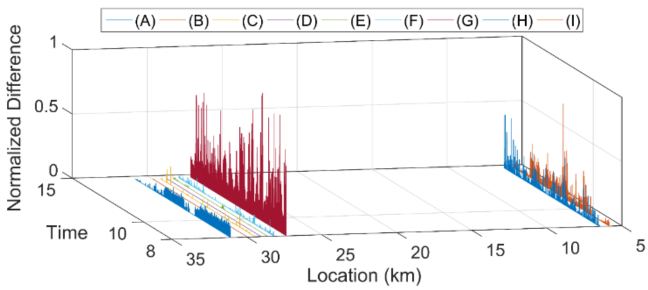


**FIGURE 3.** The normalized differences of the back-scattered light intensity detected by $\varphi$-OTDR vs time at different positions.

where $D_{Ni}$ refers to the normalized difference.

The normalized differences of the back-scattered light intensity detected by $\varphi$-OTDR from 8:00 to 14:30 at different positions are shown in Fig. 3.

In order to prove the feasibility of the principle prototype FANG, we utilize a simple method to obtain the threshold in the field test. The average value of the back-scattered light intensity in each sensing zone collected in the static condition (without a certain vibration) in 2 minutes is multiplied by a threshold coefficient of 2.25 as the threshold of the every sensing zone. It means that if the normalized difference in a sensing zone is larger than the average value in the static condition, a vibration event is considered to happen in this sensing zone. The normalized difference and the threshold of different positions are illustrated in Fig. 4 in detail. It is worth noting that the fluctuation of differences and thresholds at different positions are caused by the fiber cable position and ground condition, which affects more or less dynamic strain induced by vibration and coupled into the sensing fiber.

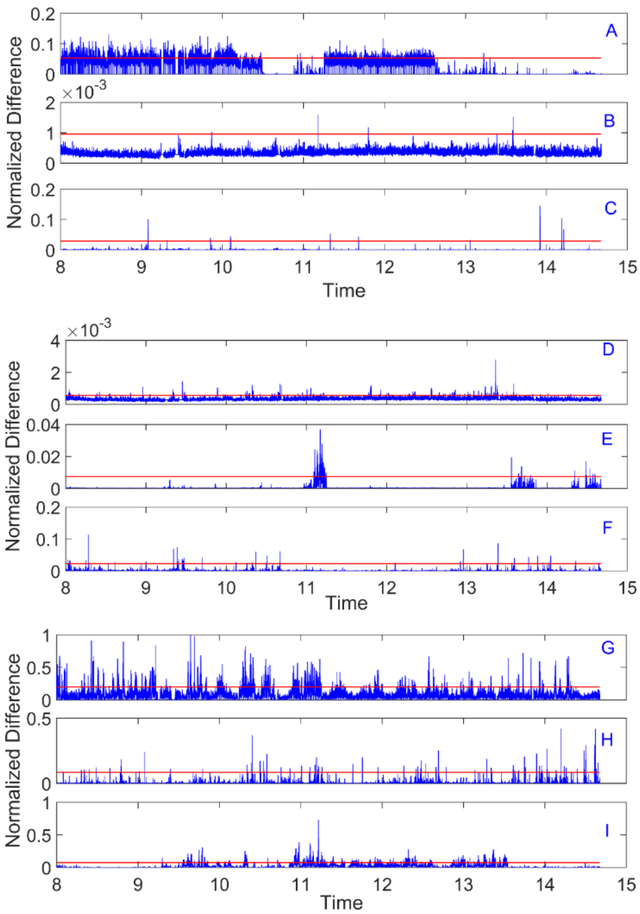


FIGURE 4. The normalized difference (blue lines) of back-scattered light intensity and the threshold (red lines) vs time at different positions.

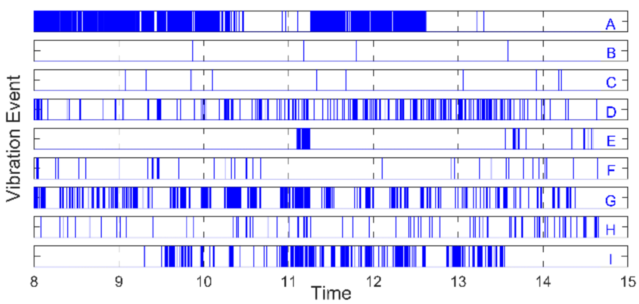


FIGURE 5. The density of vibration events vs time at different positions.

By the threshold judgment, the density of the vibration events at different positions is obtained, as shown in Fig. 5.

The temporal distribution of the vibration-event density can be considered to be three categories. Firstly, for the positions A and E, there are very dense vibration events due to the ground conditions of the mechanical working in a factory and a working rammer. Then, for the positions B and C, very few vibrations are detected. The reason is that the quiet environments passing through a forest and near a farmland. Finally, there are frequent dense vibration events at positions D, F, G, H, and I, which are respectively caused

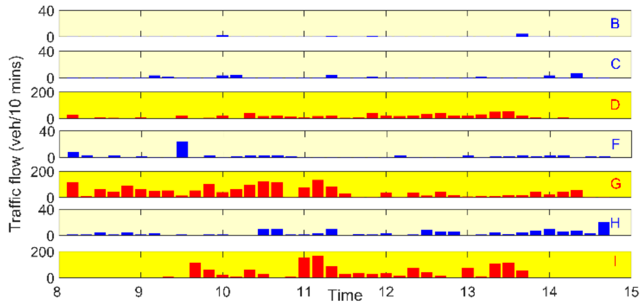


FIGURE 6. The estimated traffic flow vs Time at different positions (Blue and red for different scales).

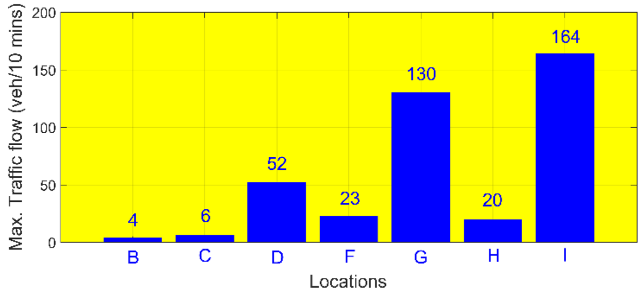


FIGURE 7. The maximal traffic flow at different positions.

by the passing vehicles on the ground conditions near a rural road, a ramp, along an express way, passing through a national highway, and along a national highway. Especially for the two positions G and I, along an express way and a national highway, the continuous high density of the vibration events are clearly observed.

For the traffic flow monitoring, the vibration events induced by the vehicles are the monitoring targets. Then, the equivalent traffic flow is obtained by calculating the amount of the vibration events in every 10 minutes, which is illustrated in Fig. 6. Furthermore, the maximal traffic flow is illustrated in Fig. 7 to present a clearly quantitative description.

It is worth noting that the highly dense vibration events due to the machine and rammer at positions A and E are removed for the traffic monitoring. Although the experimental results at positions of A and E cannot be used directly to describe the traffic flow, the vibration events observed there can reflect the operation of the factory, and the special construction situation, such as a working rammer. The results are useful for the security monitoring of the ground in a wide area.

In the cases of B and C, the traffic flow is very small, and the maximum value is only 4 and 6 per 10 minutes, which means that there are only few agricultural vehicles passing through the forest and farmland. The traffic flows at positions of F and H are higher, with the maximal value of 23 and 20 vehicles/10 mins. The position F is near a ramp, where only few vehicles pass, and the maximum traffic flow appears at 9:30 am. At the position of H, the traffic flow represents the vehicles passing through the intersection point of a national highway and the sensing fiber. A set of data on peak traffic flow is observed in the ground conditions of D, G and I, with the maximal traffic flow of 52, 130 and 164 vehicles /10 mins, respectively.

The position D is near a rural road, which is the only way to the express way. Therefore, there is a higher traffic flow at position of D than that of B, C, F, and H positions.

The positions G and I respectively along an express way and a national highway result in the highest traffic flow.

It is worth noting that the errors induced by the repeated counting of the vehicles at the same position during the collecting time have not been calibrated by the video monitoring in our field test. However, the results of traffic flow can be considered to be in an acceptable range. The value magnitudes and differences among the positions and fluctuation trends of the traffic flow at different positions are useful to reflect the traffic situation and predict the unexpected traffic accident in the huge area of suburb without the video monitoring. This is the significance of this research. In the vast area without video monitoring, it is the underground fiber cable that is the only solution to detect traffic flow.

Furthermore, we believe that the types of vehicles (diesel or gasoline engine) and road conditions (smooth or tortuous) can be obtained through AI and machine learning by collecting a large number of vibration samples in the future.

## IV. CONCLUSION

A novel FANG is proposed based on the DVS, which is realized with the help of $\varphi$-OTDR. The field test is implemented by using one of the 31.8 km-long redundant optical fibers of the buried telecom fiber cable to prove the feasibility and effectiveness for the traffic flow monitoring. The vibration events at 9 observable positions along the sensing fiber have been detected by a threshold judgement from 8:00 to 14:30. The operating machines in a factory and a working rammer are extracted at two positions. Then, the traffic flow passing through different areas and roads are estimated by the vibration-counting at different positions during 6.5 hours. For proof of concept, the estimation errors are believed to be in an acceptable range without the calibration by videos. The distribution and the fluctuation trend are useful and enlightening for the smart traffic and pre-warning of special events such as an accident. The accuracy can be improved by AI methods in the future. It seems that this work opens a new era to use telecom fiber to realize auditory nerve of ground in the suburb, which is a perfect fit to smart ground and traffic applications in the near future.

## REFERENCES

[1] S. A. Shah, D. Z. Seker, M. M. Rathore, S. Hameed, S. Ben Yahia, and D. Draheim, "Towards disaster resilient smart cities: Can Internet of Things and big data analytics be the game changers?" *IEEE Access*, vol. 7, pp. 91885–91903, 2019.

[2] H. El-Sayed, M. Chaqfa, S. Zeadally, and D. Puthal, "A traffic-aware approach for enabling unmanned aerial vehicles (UAVs) in smart city scenarios," *IEEE Access*, vol. 7, pp. 86297–86305, 2019.

[3] H. Li, Y. Liu, Z. Qin, H. Rong, and Q. Liu, "A large-scale urban vehicular network framework for IoT in smart cities," *IEEE Access*, vol. 7, pp. 74437–74449, 2019.

[4] D. Wang, B. Bai, K. Lei, W. Zhao, Y. Yang, and Z. Han, "Enhancing information security via physical layer approaches in heterogeneous IoT with multiple access mobile edge computing in smart city," *IEEE Access*, vol. 7, pp. 54508–54521, 2019.

[5] A. Murk, W. Malik, I. Mahmood, N. Ahmed, and Z. Anwar, "Big data in motion: A vehicle-assisted urban computing framework for smart cities," *IEEE Access*, vol. 7, pp. 55951–55965, 2019.

[6] X. Pan, W. Zhou, Y. Lu, and N. Sun, "Prediction of network traffic of smart cities based on DE-BP neural network," *IEEE Access*, vol. 7, pp. 55807–55816, 2019.

[7] M. A. Rodriguez-Hernandez, A. Gomez-Sacristan, and D. Gomez-Cuadrado, "SimulCity: Planning communications in smart cities," *IEEE Access*, vol. 7, pp. 46870–46884, 2019.

[8] B. Pawłowicz, M. Salach, and B. Trybus, "Smart city traffic monitoring system based on 5G cellular network, RFID and machine learning," in *Proc. Eng. Softw. Syst., Res. Praxis (KKIO)*. Pułtusk, Poland: Springer-Verlag, 2018, pp. 151–165.

[9] J. Barthélemy, N. Verstaevel, H. Forehead, and P. Perez, "Edge-computing video analytics for real-time traffic monitoring in a smart city," *Sensors*, vol. 19, no. 9, p. 2048, May 2019.

[10] R. Ke, Z. Li, J. Tang, Z. Pan, and Y. Wang, "Real-time traffic flow parameter estimation from uav video based on ensemble classifier and optical flow," *IEEE Trans. Intell. Transp. Syst.*, vol. 20, no. 1, pp. 54–64, Jan. 2019.

[11] Y. Chen, Y. Lv, X. Wang, L. Li, and F. Wang, "Detecting traffic information from social media texts with deep learning approaches," *IEEE Trans. Intell. Transp. Syst.*, vol. 20, no. 8, pp. 3049–3058, Aug. 2019.

[12] A. Fomin and S. Braeunig, "A wireless sensor system for traffic flow detection based on measurement of earth's magnetic field changes," in *Proc. 8th Medit. Conf. Embedded Comput. (MECO)*, Budva, Montenegro, Jun. 2019, pp. 1–4.

[13] K. Zheng, E. Yao, J. Zhang, and Y. Zhang, "Traffic flow estimation on the expressway network using toll ticket data," *IET Trans. Intell. Transp. Syst.*, vol. 13, no. 5, pp. 886–895, May 2019.

[14] H. Shuai and C. A. David, "Effective vehicle tracking algorithm for smart traffic networks," in *Proc. 13th IEEE Int. Conf. Service-Oriented Syst. Eng. (SOSE) 10th Int. Workshop Joint Cloud Comput. (JCC) IEEE Int. Workshop Cloud Comput. Robot. Syst. (CCRS)*, May 2019, pp. 67–76.

[15] L. Castanheira, R. Parizotto, and A. E. Schaeffer-Filho, "FlowStalker: Comprehensive traffic flow monitoring on the data plane using P4," in *Proc. IEEE Int. Conf. Commun. (ICC)*, Shanghai, China, May 2019, pp. 1–6.

[16] B. Mikhail, K. Adil, K. A. Masood, and A. Muhammad, "Accident recognition via 3D CNNs for automated traffic monitoring in smart cities," in *Proc. Comput. Vis. Conf. (CVC)*. Las Vegas, NH, USA: Springer-Verlag, 2019, pp. 256–264.

[17] Y. Djenouri, A. Belhadi, J. C.-W. Lin, and A. Cano, "Adapted K-nearest neighbors for detecting anomalies on spatio-temporal traffic flow," *IEEE Access*, vol. 7, pp. 10015–10027, 2019.

[18] C.-L. Lan and G.-L. Chang, "Empirical observations and formulations of tri-class traffic flow properties for design of traffic signals," *IEEE Trans. Intell. Transp. Syst.*, vol. 20, no. 3, pp. 830–842, Mar. 2019.

[19] C. Li and Y. Wu, "Application of improved wavelet neural network in traffic prediction of smart substation," in *Proc. Int. Conf. Intell. Comput., Commun. Devices (ICCD)*. Shenzhen, China: Springer-Verlag, 2017, pp. 1245–1254.

[20] Y. Chen, M. Guizani, Y. Zhang, L. Wang, N. Crespi, G. M. Lee, and T. Wu, "When traffic flow prediction and wireless big data analytics meet," *IEEE Netw.*, vol. 33, no. 3, pp. 161–167, May/Jun. 2019.

[21] H.-F. Yang, T. S. Dillon, E. Chang, and Y.-P. P. Chen, "Optimized configuration of exponential smoothing and extreme learning machine for traffic flow forecasting," *IEEE Trans. Ind. Informat.*, vol. 15, no. 1, pp. 23–34, Jan. 2019.

[22] X. Feng, X. Ling, H. Zheng, Z. Chen, and Y. Xu, "Adaptive multi-kernel SVM with spatial–temporal correlation for short-term traffic flow prediction," *IEEE Trans. Intell. Transp. Syst.*, vol. 20, no. 6, pp. 2001–2013, Jun. 2019.

[23] Y. Lin, X. Dai, L. Li, and F.-Y. Wang, "Pattern sensitive prediction of traffic flow based on generative adversarial framework," *IEEE Trans. Intell. Transp. Syst.*, vol. 20, no. 6, pp. 2395–2400, Jun. 2019.

[24] J. Mackenzie, J. F. Roddick, and R. Zito, "An evaluation of HTM and LSTM for short-term arterial traffic flow prediction," *IEEE Trans. Intell. Transp. Syst.*, vol. 20, no. 5, pp. 1847–1857, May 2019.

[25] M. C. R. Murça and R. J. Hansman, "Identification, characterization, and prediction of traffic flow patterns in multi-airport systems," *IEEE Trans. Intell. Transp. Syst.*, vol. 20, no. 5, pp. 1683–1696, May 2019.

[26] T. Pamuła, "Impact of data loss for prediction of traffic flow on an urban road using neural networks," *IEEE Trans. Intell. Transp. Syst.*, vol. 20, no. 3, pp. 1000–1009, Mar. 2019.

[27] T. Zhou, D. Jiang, Z. Lin, G. Han, X. Xu, and J. Qin, "Hybrid dual Kalman filtering model for short-term traffic flow forecasting," *IET Intell. Transp. Syst.*, vol. 13, no. 6, pp. 1023–1032, 2019.

[28] X. Hu, X. Wei, Y. Gao, W. Zhuang, M. Chen, and H. Lv, "An attention-mechanism-based traffic flow prediction scheme for smart city," in *Proc. 15th Int. Wireless Commun. Mobile Comput. Conf. (IWCMC)*, Tangier, Morocco, Jun. 2019, pp. 1822–1827.

[29] S. Zhang, Z. Kang, Z. Zhang, C. Lin, C. Wang, and J. Li, "A hybrid model for forecasting traffic flow: Using layerwise structure and Markov transition matrix," *IEEE Access*, vol. 7, pp. 26002–26012, 2019.

[30] F. Anilloy, K. A. Aamri, Y. Salim, and Z. Amer, "IoT based smart traffic density control using image processing," in *Proc. 4th MEC Int. Conf. Big Data Smart City (ICBDSC)*, Feb. 2019, pp. 1–4.

[31] P. Bartosz, S. Mateusz, and T. Bartosz, "Infrastructure of RFID-based smart city traffic control system," in *Prog. Automat., Robot. Meas. Techn., Outcomes Int. Conf. (AUTOMATION)*. Warsaw, Poland: Springer-Verlag, Mar. 2019, pp. 186–198.

[32] M. Lingani Guy, B. Rawat Danda, and G. Moses, "Smart traffic management system using deep learning for smart city applications," in *Proc. IEEE 9th Annu. Comput. Commun. Workshop Conf. (CCWC)*, Mar. 2019, pp. 101–106.

[33] S. Schiller, "Feasibility of giant fiber-optic gyroscopes," *Phys. Rev. A, Gen. Phys.*, vol. 87, no. 3, Mar. 2013, Art. no. 033823.

[34] C. Clivati, D. Calonico, G. A. Costanzo, A. Mura, M. Pizzocaro, and F. Levi, "Large-area fiber-optic gyroscope on a multiplexed fiber network," *Opt. Lett.*, vol. 38, no. 7, pp. 1092–1094, Apr. 2013.

[35] M. Bourmpos, A. Argyris, and D. Syvridis, "Smart city surveillance through low-cost fiber sensors in metropolitan optical networks," *Fiber Integr. Opt.*, vol. 33, no. 3, pp. 205–223, 2014.

[36] H. Wu, S. Xiao, X. Li, Z. Wang, J. Xu, and Y. Rao, "Separation and determination of the disturbing signals in phase-sensitive optical time domain reflectometry ($\phi$-OTDR)," *J. Lightw. Technol.*, vol. 33, no. 15, pp. 3156–3162, Aug. 1, 2015.

[37] Y. Wu, Z. Wang, J. Xiong, J. Jiang, S. Lin, and Y. Chen, "Interference fading elimination with single rectangular pulse in $\phi$-OTDR," *J. Lightw. Technol.*, vol. 37, no. 13, pp. 3381–3387, May 14, 2019.

[38] Y. Fu, N. Xue, Z. Wang, B. Zhang, J. Xiong, and Y. Rao, "Impact of I/Q amplitude imbalance on coherent $\phi$-OTDR," *J. Lightw. Technol.*, vol. 36, no. 4, pp. 1069–1075, Feb. 15, 2018.

[39] M. Zabihi, Y. Chen, T. Zhou, J. Liu, Y. Shan, Z. Meng, F. Wang, Y. Zhang, X. Zhang, and M. Chen, "Continuous fading suppression method for $\phi$-OTDR systems using optimum tracking over multiple probe frequencies," *J. Lightw. Technol.*, vol. 37, no. 14, pp. 3602–3610, Jul. 15, 2019.

[40] J. Li, Z. Zhang, J. Gan, Z. Zhang, X. Heng, K. Zhou, H. Zhao, S. Xu, and Z. Yang, "Influence of laser linewidth on phase-OTDR system based on heterodyne detection," *J. Lightw. Technol.*, vol. 37, no. 14, pp. 2641–2647, Jul. 1, 2019.

[41] G. Yang, X. Fan, Q. Liu, and Z. He, "Frequency response enhancement of direct-detection phase-sensitive OTDR by using frequency division multiplexing," *J. Lightw. Technol.*, vol. 36, no. 4, pp. 1197–1203, Feb. 15, 2018.

[42] Z. Zhong, F. Wang, M. Zong, Y. Zhang, and X. Zhang, "Dynamic measurement based on the linear characteristic of phase change in $\Phi$-OTDR," *IEEE Photon. Technol. Lett.*, vol. 31, no. 14, pp. 1191–1194, Jul. 15, 2019.

[43] H. Jia, S. Liang, S. Lou, and X. Sheng, "A $\kappa$-nearest neighbor algorithm-based near category support vector machine method for event identification of $\varphi$-OTDR," *IEEE Sensors J.*, vol. 19, no. 10, pp. 3683–3689, May 2019.

[44] G.-M. Ma, C. Shi, W.-Q. Qin, Y.-B. Li, H.-Y. Zhou, and C.-R. Li, "A non-intrusive electrical discharge localization method for gas insulated line based on phase-sensitive OTDR and michelson interferometer," *IEEE Trans. Power Del.*, vol. 34, no. 4, pp. 1324–1331, Aug. 2019.

[45] X. Wang, B. Lu, Z. Wang, H. Zheng, J. Liang, L. Li, Q. Ye, R. Qu, and H. Cai, "Interference-fading-free $\phi$-OTDR based on differential phase shift pulsing technology," *IEEE Photon. Technol. Lett.*, vol. 31, no. 1, pp. 39–42, Jan. 1, 2019.

[46] Y. Wu, S. Liang, S. Lou, and X. Sheng, "An interrogation method to enhance SNR for far-end disturbances in fiber-optic distributed disturbance sensor based on $\varphi$-OTDR," *IEEE Sensors J.*, vol. 19, no. 3, pp. 1064–1072, Feb. 2019.

[47] N. Xue, Y. Fu, C. Lu, J. Xiong, L. Yang, and Z. Wang, "Characterization and compensation of phase offset in $\Phi$-OTDR with heterodyne detection," *J. Lightw. Technol.*, vol. 36, no. 23, pp. 5481–5487, Dec. 1, 2018.

[48] Z. Zhong, F. Wang, and X. Zhang, "Event discrimination using phase correlation in $\Phi$-OTDR system based on coherent detection," *IEEE Photon. J.*, vol. 10, no. 5, Oct. 2018, Art. no. 7104508.

[49] X. He, M. Zhang, S. Xie, F. Liu, L. Gu, and D. Yi, "Self-referenced accelerometer array multiplexed on a single fiber using a dual-pulse heterodyne phase-sensitive OTDR," *J. Lightw. Technol.*, vol. 36, no. 14, pp. 2973–2979, Jul. 15, 2018.

[50] H. Liu, F. Pang, L. Lv, X. Mei, Y. Song, J. Chen, and T. Wang, "True phase measurement of distributed vibration sensors based on heterodyne $\Phi$-OTDR," *IEEE Photon. J.*, vol. 10, no. 1, Feb. 2018, Art. no. 7101309.

[51] C. Wang, Y. Shang, W.-A. Zhao, X.-H. Liu, C. Wang, and G.-D. Peng, "Investigation and comparison of $\varphi$-OTDR and OTDR-interferometry via phase demodulation," *IEEE Sensors J.*, vol. 18, no. 4, pp. 1501–1505, Feb. 2018.

[52] C. Cao, F. Wang, Y. Pan, X. Zhang, X. Chen, Q. Chen, and J. Lu "Suppression of signal fading with multi-wavelength laser in polarization OTDR," *IEEE Photon. Technol. Lett.*, vol. 29, no. 21, pp. 1824–1827, Nov. 1, 2017.

[53] Z. Sha, H. Feng, Y. Shi, W. Zhang, and Z. Zeng, "Phase-sensitive OTDR with 75-km single-end sensing distance based on RP-EDF amplification," *IEEE Photon. Technol. Lett.*, vol. 29, no. 16, pp. 1308–1311, Aug. 15, 2017.

[54] H. He, L. Shao, H. Li, W. Pan, B. Luo, X. Zou, and L. Yan, "SNR enhancement in phase-sensitive OTDR with adaptive 2-D bilateral filtering algorithm," *IEEE Photon. J.*, vol. 9, no. 3, Jun. 2017, Art. no. 6802610.

[55] X. Zhang, Z. Sun, Y. Shan, Y. Li, F. Wang, J. Zeng, and Y. Zhang, "A high performance distributed optical fiber sensor based on $\Phi$-OTDR for dynamic strain measurement," *IEEE Photon. J.*, vol. 9, no. 3, Jun. 2017, Art no. 6802412.

[56] G. Tu, B. Yu, S. Zhen, K. Qian, and X. Zhang, "Enhancement of signal identification and extraction in a $\Phi$-OTDR vibration sensor," *IEEE Photon. J.*, vol. 9, no. 1, Feb. 2017, Art. no. 7100710.

[57] Y. Wang, B. Jin, Y. Wang, D. Wang, X. Liu, and Q. Bai, "Real-time distributed vibration monitoring system using $\Phi$-OTDR," *IEEE Sensors J.*, vol. 17, no. 5, pp. 1333–1341, Mar. 2017.

[58] N. J. Lindsey, E. R. Martin, D. S. Dreger, B. Freifeld, S. Cole, S. R. James, B. L. Biondi, and J. B. Ajo-Franklin, "Fiber-optic network observations of earthquake wavefields," *Geophys. Res. Lett.*, vol. 44, no. 23, pp. 11792–11799, Dec. 2017.

[59] G. A. Wellbrock, T. J. Xia, M.-F. Huang, Y. Chen, M. Salemi, Y.-K. Huang, P. Ji, E. Ip, and T. Wang, "First field trial of sensing vehicle speed, density, and road conditions by using fiber carrying high speed data," in *Proc. Opt. Fiber Commun. Conf. Exhib. (OFC)*, San Diego, CA, USA, 2019, pp. 1–3.


**SHENG LIANG** received the Ph.D. degree in precision instrument and machinery from Beihang University, Beijing, China, in 2011. He is currently an Associate Professor with the Department of Physics, School of Science, Beijing Jiaotong University, Beijing. His research interests include fiber-optic sensors, microstructured optical fibers, and photonics.

**XIAOTING ZHAO** received the bachelor's degree in computer science and technology from Anhui Agricultural University, Anhui, China, in 2019. He is currently pursuing the Ph.D. degree with Beijing Jiaotong University. His research interests include fiber-optic sensors and microstructured optical fibers.

**RUIJUN LIU** received the M.S. degree from Beihang University, in 2009, and the Ph.D. degree from the Ecole Centrale de Nantes, France, in 2013. He is currently with Beijing Technology and Business University. His current research interests include machine learning, virtual reality, and 3-D reconstruction.

**XIAODONG ZHANG** received the master's degree in transportation engineering from Jilin University, Jilin, China, in 2004. He is currently a Full Professor with the Department of Information Center, Beijing Municipal Institute of City Planning and Design, Beijing, China. His research interests include smart city transportation planning and complex systems.

**LIANG WANG** received the master's degree in computational mathematics from Beijing Normal University, Beijing, China, in 2015. He is currently an Engineer with the Department of Information Center, Beijing Municipal Institute of City Planning and Design, Beijing, China. His research interests include smart city, big data, and complex systems.

**XINGHUA ZHANG** received the Ph.D. degree from the Chinese Academy of Science. He was as a Postdoctoral Researcher with Colorado State University, USA. He is currently an Associate Professor with the Department of Physics, School of Science, Beijing Jiaotong University. His research interests include statistical physics, complex systems, and soft matter.

**YISHENG LV** received the B.E. and M.E. degrees in transportation engineering from the Harbin Institute of Technology, Harbin, China, in 2005 and 2007, respectively, and the Ph.D. degree in control theory and control engineering from the Chinese Academy of Sciences, in 2010. He is currently an Associate Professor with the Institute of Automation, Chinese Academy of Sciences. His research interests include traffic data analysis, dynamic traffic modeling, and parallel traffic management and control systems.

**FANCHAO MENG** received the master's degree in optical engineering from Yanshan University, Hebei, China, in 2019. He is currently pursuing the Ph.D. degree with Beijing Jiaotong University. His research interests include fiber-optic sensors and microstructured optical fibers.